



# AirCargoChallenge 2022

# Technical Report

Team #20

HUSZ Falcon – EUROAVIA Zagreb



# CONTENTS

---

1. INTRODUCTION .....	4
1.1 EUROAVIA ZAGREB AND AIR CARGO CHALLENGE.....	4
1.2 METHODOLOGY .....	5
2. PROJECT MANAGEMENT.....	6
2.1 TEAM STRUCTURE .....	6
2.2 TIME SCHEDULE .....	7
2.3 FINANCES.....	7
3. PRELIMINARY SIZING.....	9
3.1 GOALS .....	9
3.2 POINTS EQUATION ANALYSIS .....	9
3.3 CONFIGURATION .....	10
3.4 WING PARAMETERS.....	11
3.5 POWERPLANT PARAMETERS .....	11
3.6 MTOW PREDICTION .....	12
3.7 DRAG POLAR.....	12
3.8 PERFORMANCE REQUIREMENTS AND MATCHING CHART .....	13
3.9 PAYLOAD PREDICTION .....	15
4. AERODYNAMIC DESIGN .....	16
4.1 WING DESIGN .....	16
4.1.1 AIRFOIL SELECTION.....	16
4.1.2 LIFT DEVICES AND CONTROL SURFACES .....	18
4.1.3 NUMERICAL ANALYSIS.....	20
4.1.4 BLENDED-WING OVERVIEW .....	21
4.2 TAIL DESIGN .....	21
5. CENTER OF GRAVITY .....	23
6. STABILITY ANALYSIS .....	24
6.1 LONGITUDINAL STABILITY.....	24
6.1.1 WING LIFT GRADIENT .....	25
6.1.2 HORIZONTAL AND VERTICAL STABILIZER LIFT GRADIENTS.....	25
6.2 DIRECTIONAL STATIC STABILITY.....	25

6.3 RESULTS .....26

7. STRUCTURAL DESIGN .....28

7.1 FUSELAGE.....28

8. OUTLOOK .....30

APPENDIX A – DRAWINGS .....31

APPENDIX B – BOUNDING BOX .....35

APPENDIX C – ADDITIONAL WEIGHT DATA.....36

APPENDIX D – NUMERICAL RESULTS.....38

Bibliography.....43

# 1. INTRODUCTION

---

## 1.1 EUROAVIA ZAGREB AND AIR CARGO CHALLENGE

EUROAVIA Zagreb is a member of EUROAVIA, and a Croatian student association oriented towards connecting aerospace students with the industry, and providing its members invaluable experience regarding aircraft design, manufacture, and testing. Therefore, as the most important activity in the association, Air Cargo Challenge has become an essential tool for learning and developing each generation of aerospace engineers in Croatia. The association has been competing at the competition since 2007, and the best result is 1<sup>st</sup> place at the competition in 2015 in Munich with aircraft *HUSZ Tern* (Figure 1.1 - HUSZ Tern). In 2017, as the previous winners, the team from Zagreb hosted a competition in Croatia (Figure 1.2). This year, EUROAVIA Zagreb will be competing with aircraft **HUSZ Falcon**.



Figure 1.1 - HUSZ Tern



Figure 1.2 - Air Cargo Challenge 2017, Zagreb

## 1.2 METHODOLOGY

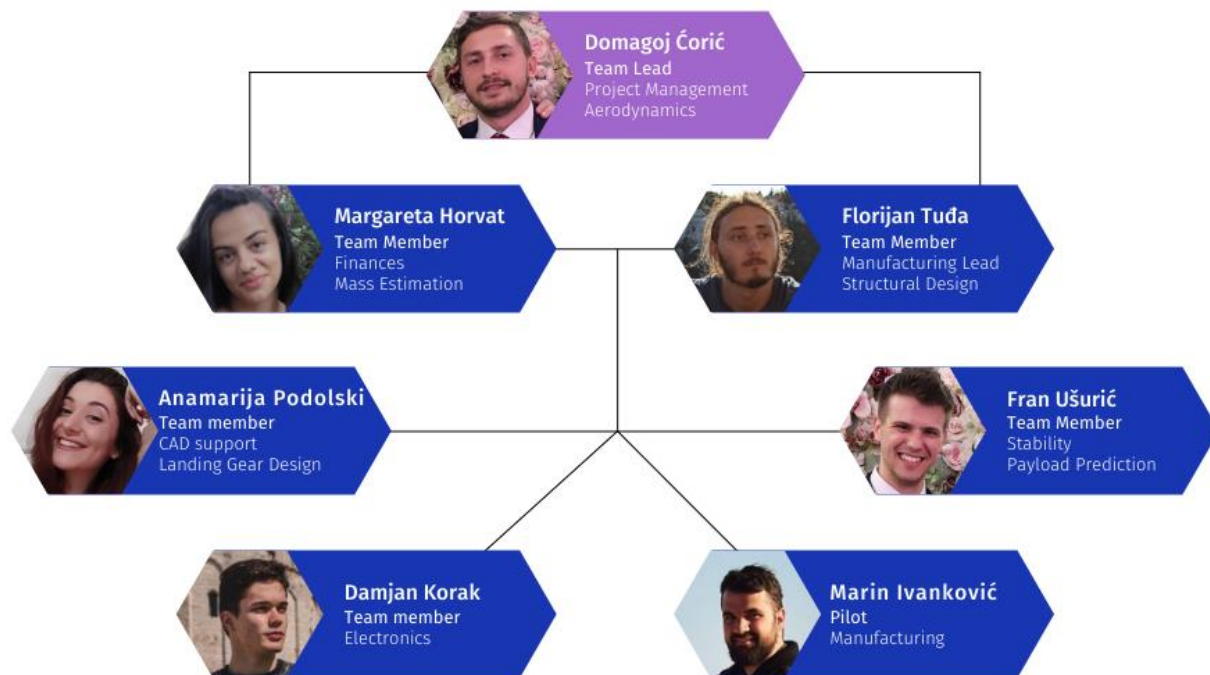
As the regulations for 2022 challenge present a real-life adaptation that refreshed current state of the competition, they also present some interesting new topics and design challenges. The design begins with detailed points analysis and payload prediction. Then preliminary sizing of the aircraft is conducted to obtain initial parameters of the aircraft that will be used for detailed design later. After preliminary sizing, aerodynamics design of the main parts begins, parallel to structural design of the complete aircraft. Soon after, the stability analysis begins, and optimization process starts. Complete design process is based on [1] and the team tried to support every design decision with analytical and/or numerical calculations with software tools such as *Matlab*, *OpenFOAM*, *XFOIL*, *Xflr5*, and *Abaqus*, while referencing to the previous experience at the competition.

## 2. PROJECT MANAGEMENT

---

### 2.1 TEAM STRUCTURE

The team consists of 7 students from the University of Zagreb, with each member having designated main task regarding design, manufacturing, piloting, and/or administration. At the beginning, a team lead for the competition has been chosen. Quickly after, at the first meeting, a meeting schedule on the weekly basis has been determined, as well as main tasks for each member. Team overview is given in the diagram below.



The project timeline has been monitored with a Gantt chart and each member has been reporting his or her tasks for the following week with technical reports and quick presentation at the meeting. Every week new sub-tasks were given in accordance with mentor. When confronted with a technical struggle, besides our mentor, team has been in contact with other association members, association alumni, professors, and engineers.

## 2.2 TIME SCHEDULE

In September 2021 the team has started with the design phase. First, the competition analysis and payload estimation were conducted. After that the aircraft configuration was chosen and this marked the beginning of preliminary sizing. Until December 2021 the preliminary sizing was done, and the team started with detailed aerodynamics and structural design of fuselage, wing, tail, and landing gear. Alongside, the mass estimation and determination of the centre of mass began, as well as manufacturing planning. In February 2022 the team finished aircraft sizing and design of main parts. Then began stability analysis with some minor corrections to the original design. Finally, until the late April, the team optimized aerodynamics and structural design, as well as started the manufacturing phase. Every design phase mentioned is given in the Figure 2.1 below.



Figure 2.1 - Project timeline

## 2.3 FINANCES

As for all technical projects, finances present one of the biggest challenges. That is the reason why the team decided on selecting a team member that will supervise all finances. This means that financial officer, in communication with all members and mentioned contacts, conducted cost analysis for every design phase. Furthermore, financial officer and team lead were also primarily responsible for contacting sponsors and applying for grants. Projected costs are given in the Table 1.

Table 1 - Costs approximation

<b>Cost type</b>	<b>Cost Value</b>
Material	2 000 €
Electronics	400 €
Manufacturing	2 500 €
Participation Fee	1 750 €
Travel Expenses	1 000 €
Other	200 €
<b>TOTAL</b>	<b>8 250 €</b>

The manufacturing presented the biggest financial issue due to the CNC milling of moulds and waterjet cutting. However, the team has found a sponsor that is willing to provide a complete tooling procedure for free which eliminated the largest cost. Additionally, other financial sponsors have been found. Current main team sponsors and their contributions are given in the Table 2.

Table 2 - Sponsorship contributions

<b>Sponsor</b>	<b>Financial Contribution</b>
Croatian Civil Aviation Agency	4 600 €
Ch-aviation	1 500 €
Grad-export	2 500 € (tooling costs)
Faculty of Mechanical Engineering and Naval Architecture Zagreb	1 300 €
PBZ	800 €
<b>TOTAL</b>	<b>10 700 €</b>

From given tables it can be noticed that all costs are already covered, and team does not have any financial issues regarding the manufacturing and travel costs.

### 3. PRELIMINARY SIZING

---

In this section, detailed sizing procedures for wing, power, and mass are shown. The process is based on [1].

#### 3.1 GOALS

The aircraft configuration is chosen based on *Analytic Hierarchy Process (AHP)* method [2] implemented in *Matlab*, therefore at the beginning of the design phase, goals for aircraft had to be determined. They were chosen according to competition regulations. The list of goals is given below:

- Flight speed maximization
- Ascent speed maximization
- Payload mass maximization
- Payload loading and unloading time minimization
- Manufacturing simplicity

Detailed explanation of goals and their hierarchy are shown in the appendix.

#### 3.2 POINTS EQUATION ANALYSIS

After a detailed analysis of the point system in *Matlab*, it can be deduced that the most points are awarded for flight speed and ascent speed. Payload mass is in second place when considering importance, whereas loading and unloading time hold 3<sup>rd</sup> place. In the Figure 3.1 the number of points with relation to distance and payload mass is given.

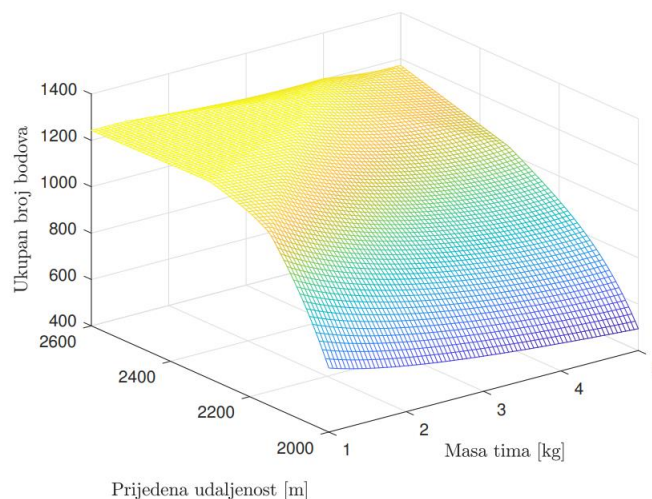


Figure 3.1 - Number of points with relation to distance and payload mass

The graph shows that maximum number of points is achieved with payload mass of 3 kg which corresponds to the flight speed of 19.667 m/s. This data is crucial for determining optimal configuration of the aircraft in the next part.

### 3.3 CONFIGURATION

This section shows the process of determining aircraft configuration. It was limited to defining wing, tail, and undercarriage of the aircraft to maintain relative simplicity in the early design phase.

Regarding the wing design, the team compared general concepts such as monoplane and flying wing, as well as wing geometry (elliptic, rectangular, swept) and position (high, mid, low). When it comes to tail, the team analyzed conventional, T-tail, and inverted V tail concepts. For undercarriage the tricycle concept was considered.

After the thorough analysis, the proposed configurations are given in the table below.

Table 3 - Proposed configurations

	Configuration 1 (C1)	Configuration 2 (C2)	Configuration 3 (C3)	Configuration 4 (C4)
<b>Wing geometry</b>	Elliptic	Swept	Swept	Flying wing
<b>Wing position</b>	High	High	High	/
<b>Tail</b>	T-tail	Inverted V	T-tail	/
<b>Undercarriage</b>	Tricycle	Tricycle	Tricycle	Tricycle

Due to the transport box dimensions, swept wing was chosen to maximize the wingspan. Furthermore, considering transportation nature of the competition and manufacturing, high positioned wings are optimal. Flying wing concept was dismantled due to lower *MTOW* values and stability issues. Only unknown was regarding tail design because after conducting *AHP* method for determination, T-tail and inverted V tail have shown similar characteristics. Thus, additional analyses were conducted for configurations C2 and C3. In the end the team decided on configuration 2. Proposed configurations are given in the Figure 3.2 - Proposed configurations (Left to right; C1, C2, C3, C4).

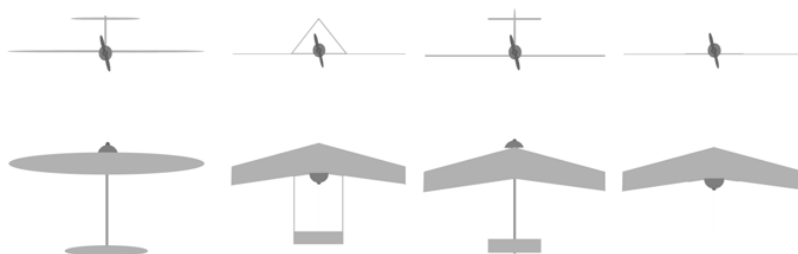


Figure 3.2 - Proposed configurations (Left to right; C1, C2, C3, C4)

### 3.4 WING PARAMETERS

According to the regulations and dimensions of the transportation box, the maximum wingspan has been chosen that fit inside a box (Appendix B). That wingspan  $b_a$  was assumed, and based on that assumption, wing area  $S_{ref}$  and wing wetted area  $S_{wet}$  have been determined for each configuration based on [1]. Table 4 shows basic wing parameters for both configurations.

Table 4 - Basic wing parameters

<b>Configuration 2</b>	
	$b_a = 2.478 \text{ m}$
	$S_{ref} = 0.43208 \text{ m}^2$
	$S_{wet} = 2.1721 \text{ m}^2$
	$AR = 14.604$

### 3.5 POWERPLANT PARAMETERS

Tables Table 5 and Table 6 show motor and propeller specifications. Based on them, the battery was chosen.

Table 5 - Motor specifications

<b>AXI 2826/10 GOLD LINE V2 [3]</b>	
Number of cells	3-5 Li-Poly
RPM/V	920
Max. efficiency	$\eta_{motor} = 0.86$
Dimensions	35x52 mm
Shaft diameter	5 mm
Weight	177 g
Max. power	740 W

Table 6 - Propeller specifications

<b>Propeller</b>	
Diameter	0.254 m
Efficiency	$\eta_{prop} = 0.85$

The real power of the motor is given by the equation below:

$$P_{ef} = P_{max} \times \eta_{prop} \times \eta_{motor} = 540.94 \text{ W}$$

The proposed battery pack for the aircraft is then given in the Table 7.

Table 7 – Battery specifications

<b>Zeee 8000 mAh 11.1 V 100C 3S [4]</b>	
Dimensions	138 x 47 x 36 mm
Weight	493 g
Capacity	8000 mAh

### 3.6 MTOW PREDICTION

Like preliminary sizing of commercial or military aircraft, the design of small electric aircraft should also begin with gathering information about similar aircraft which will help with initial assumptions. Empty and take-off weights of similar aircraft that were used to plot mass regression line (Appendix C) based on equation 1 in *Matlab* are given in the appendix.

$$\log_{(10)}W_{(E)} = \frac{1}{B} \log_{(10)}W_{(TO)} - \frac{A}{B} \quad (1)$$

where A and B are linear coefficients based on similar aircraft. For this case, coefficients are:

- $A = -0.0193$ ,  $B = 1.7580$

The projected empty weight is based on assuming  $W_{TO} = 7.14$  kg, which consists of battery weight (0.463 kg), motor weight (0.177 kg), with assumed aircraft weight based on experience (2.5 kg), and maximum payload (4 kg). This results in  $W_E = 3.29$  kg.

### 3.7 DRAG POLAR

Drag polar is determined according to [5] and is shown in Figure 3.3. The initial parameters are:

1. Wetted area is  $S_{wet} = 2.1721$  m<sup>2</sup> and take-off mass is  $m_{TO} = 7.14$  kg. Wing loading during take-off is assumed according to similar aircraft;  $\frac{W_{(TO)}}{S} = 10$ .
2. Equivalent friction coefficient  $c_f$  is assumed from tables in [5]. The chosen coefficient is 0.01 which fits smaller and slower aircraft.
3. Equivalent parasitic area  $f$  is given by equation  $\log_f = a + b * \log_{10}(S_{wet})$
4. Aspect ratio was assumed according to similar aircraft and preliminary CAD model. Oswald coefficient is assumed according to [5] as  $e_{clean} = 0.85$  and  $e_{TO} = 0.8$ .
5. Zero-lift drag coefficient is  $C_{D0} = \frac{f}{S}$ , and coefficient  $K$  is  $K = \frac{1}{\pi e A}$ .
6. Drag coefficient additions due to landing gear and flaps are added;  $C_{D0,lg} = 0.015$  and  $C_{D0,flaps} = 0.015$ .

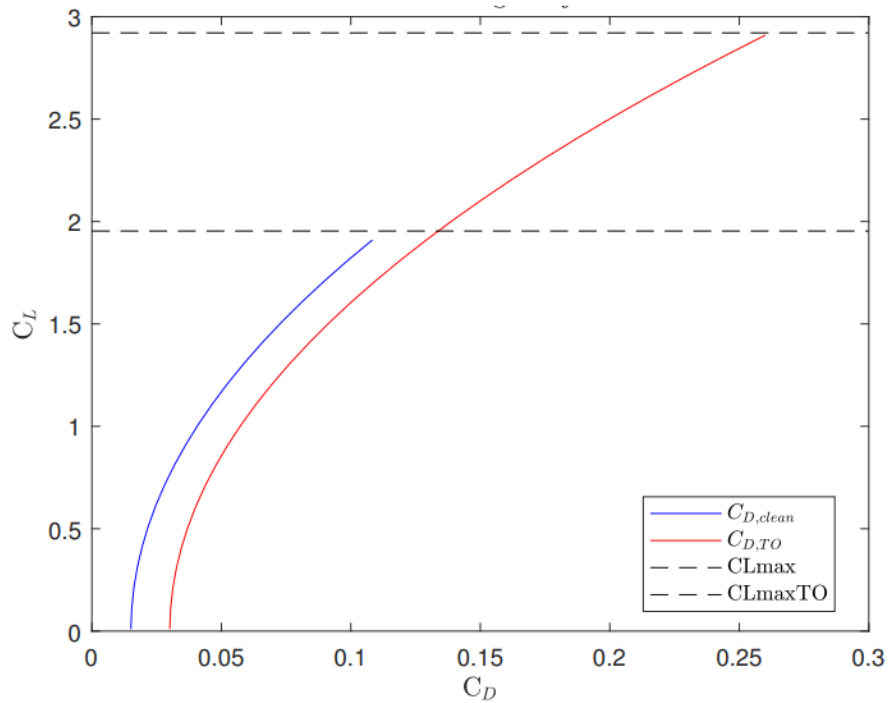


Figure 3.3 - Drag polar

Drag polar function is given below:

$$\begin{aligned} C_{D,clean} &= 0.0151 + 0.0256C_L^2 \\ C_{D,TO} &= 0.0301 + 0.0272C_L^2 \end{aligned} \quad (2)$$

### 3.8 PERFORMANCE REQUIREMENTS AND MATCHING CHART

The next step in conceptual design phase is to plot a matching chart and determine optimal wing loading and power loading. The performance requirements are determined according to flight competition rules, and they are:

- Take-off distance
- Turn radius
- Landing ( $V_{stall}$ )
- Horizontal flight speed

Matching chart is dependable of wing loading  $W/S$  and power loading  $W/P$ . Wing loading can be determined by previous calculations, whereas power loading is determined by  $m_{to}$  and available power  $P_a$  that is calculated in *Matlab*. The matching chart for this aircraft is given in Figure 3.4 and aircraft performance is given in the

Table 7.

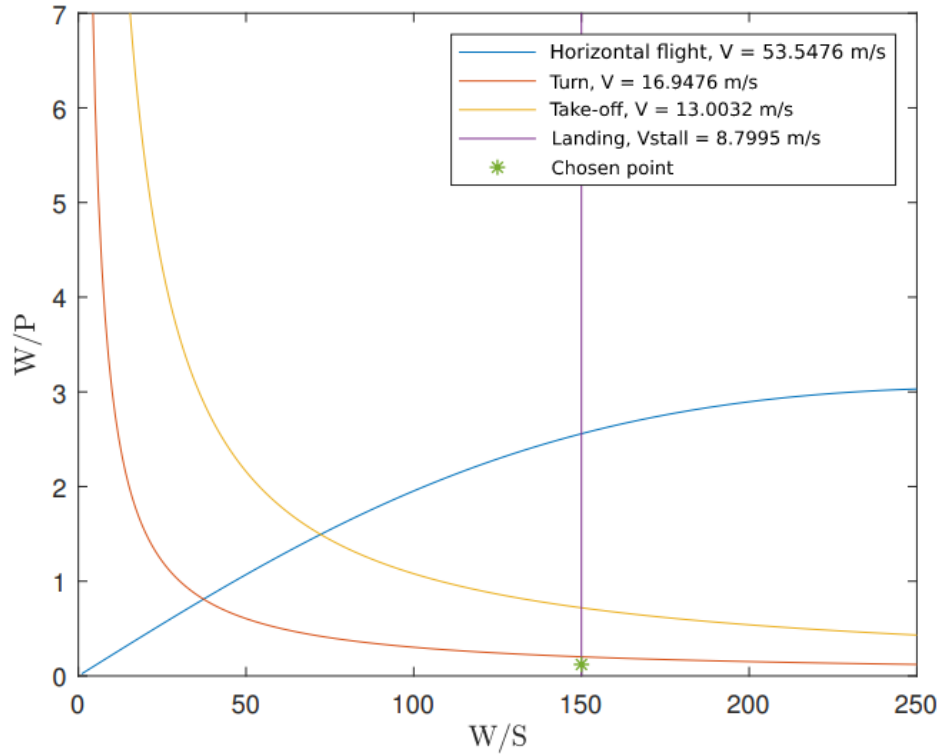


Figure 3.4 - Matching chart

Table 7 - Aircraft performance

$V_{max}$ [m/s]	55.6176
$V_{turn}$ [m/s]	12.3376
$V_{TO}$ [m/s]	13.0032
$V_{stall,cruise}$ [m/s]	11.1966
$V_{stall,landing}$ [m/s]	8.7995
$V_{stall,TO}$ [m/s]	9.1566
$R_{min}$ [m]	13.5590
$L_{TO}$ [m]	15.4150

Now the points prediction can be generated, and this configuration produces **1126.7** points according to the points equation.

### 3.9 PAYLOAD PREDICTION

The payload weight is calculated as difference between total lift (expressed in kilograms) and empty weight of the aircraft. As the payload prediction needs to be expressed as a linear model, the following formula is used:

$$L = 0.5 * \rho * V^2 * S_{wing} * C_L \quad (2)$$

$$PL = L - W_E$$

while the density is calculated as:

$$\rho = 0.003484 * \frac{p}{T}$$

Where:

$$p = 101325 * (1 - 0.00002256 * h)^{5.256}$$

$$T = 288.15 - 0.0065 * h$$

The parameters in equation 2 can be obtained by calculations before and from section 4. The payload prediction function is given in relation to altitude in Figure 3.5. The linear payload prediction function is:

$$PL = 4.1643 - 0.0007 * h$$

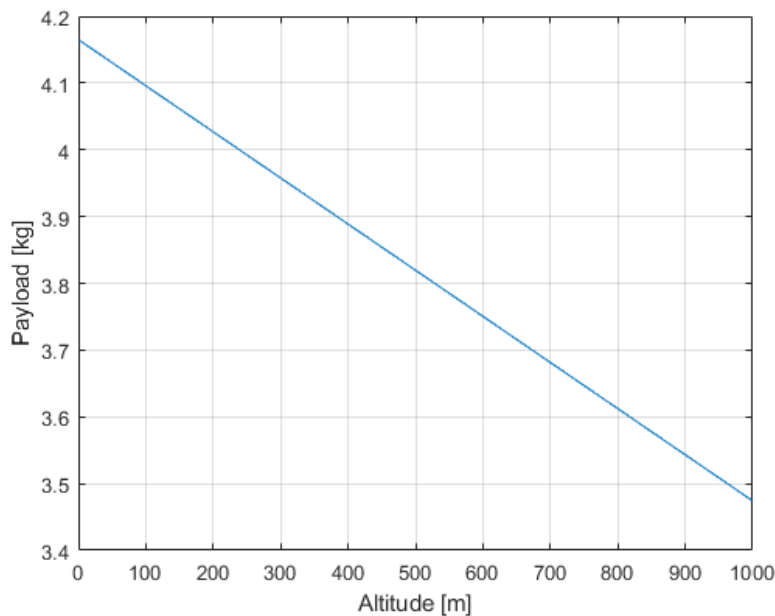


Figure 3.5 - Payload prediction

## 4. AERODYNAMIC DESIGN

---

### 4.1 WING DESIGN

After successfully acquiring a matching chart for the aircraft, wing area and aspect ratio can be determined:

- Wing area:  $S = 0.3932 \text{ m}^2$
- Aspect ratio:  $AR = 14.65$

As the aircraft is blended-wing type, the wingspan is including the span of fuselage too and is given below:

$$b = \sqrt{(AR * S)} = 2.4 \text{ m} \quad (3)$$

Taper ratio  $\lambda$  has contradictory requirements from structural design point and aerodynamics point. Lower ratio means lighter aircraft and better aerodynamic loading. On the other hand, lower  $\lambda$  present higher chance of airflow detachment on wingtips, which effects ailerons performance. It is known that ideal wing, by the means of minimum induced drag, is elliptical wing. It is complicated from the structural design point of view; therefore, it is not common. However, the taper ratio can be modified so that the wing can be as similar to elliptical wing as possible ( $\lambda \approx 0.3$ ). Thus, according to similar aircraft and research [6] [7], chosen taper ratio is  $\lambda=0.6$ . Now, the wingtip and root airfoil chords can be calculated:

- $c_r = 200 \text{ mm}$
- $c_t = 120 \text{ mm}$

#### 4.1.1 AIRFOIL SELECTION

One of the main goals for this aircraft is to maximize the payload weight. Therefore high-lift, low Reynolds number airfoils are considered. They generate high lift values but have larger induced drag. Furthermore, they operate at lower  $Re$  numbers which means that they have a tendency of flow detachment over the upper surface of the wing.

4 airfoils are chosen, and each one has been analyzed in *XFOIL* [8] and *XFLR5* for the range of angles of attack  $\alpha \in [-10^\circ, 20^\circ]$  and the lowest  $Re$  number during the flight ( $Re = 1,4418 \times 10^5$ ) which corresponds to stall speed during the landing. The assumption is that for higher  $Re$  numbers, the airfoils will only produce better results.

The analyzed airfoils are:

- CH10 (smoothed)
- FX 74-C15-140 MOD (smoothed)
- S1210 12%
- S1223

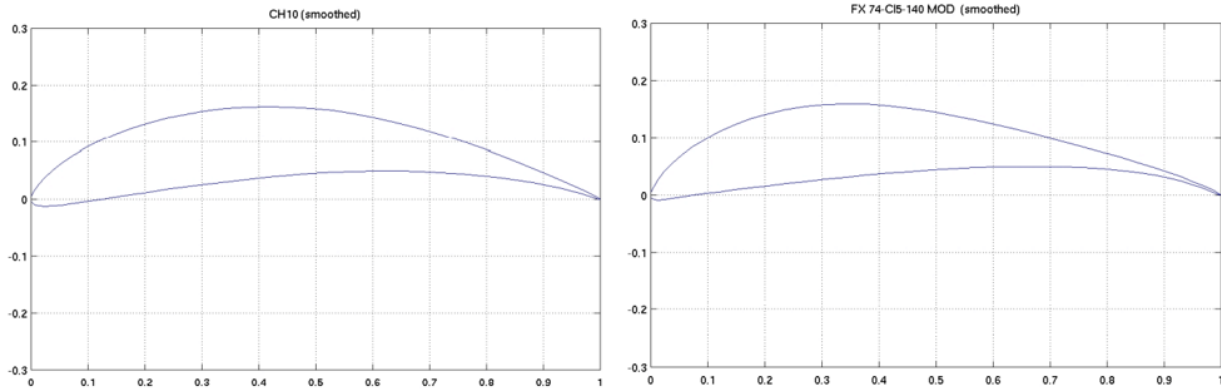


Figure 4.1 - Airfoils CH-10 (left) and FX 74-C15-140 MOD (right)

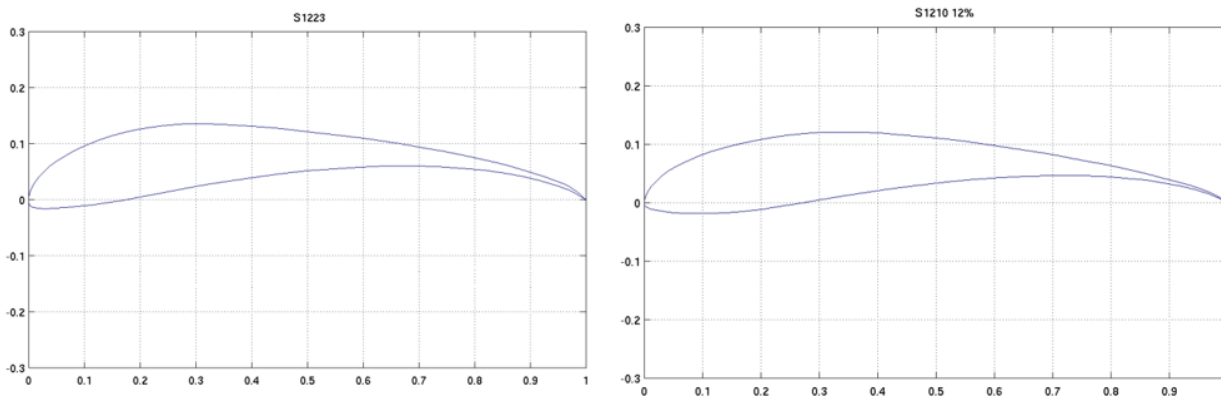


Figure 4.2 - Airfoils S1223 (left) and S1210 12% (right)

The wing, in its pure form, needs to meet the requirements for maximum cruise lift coefficient, which has been already determined with drag polar ( $C_{L,max} = 1.95$ ). From the Figure 4.3 it can be seen that only airfoils S1223 and S1210 meet the required  $C_{L,max}$ . To choose the optimal airfoil, additional calculations for all characteristic  $Re$  numbers need to be conducted and required airfoil lift coefficient needs to be calculated. The required airfoil lift coefficient is based on maximum cruise lift coefficient with additional corrections imposed on it, such as tail effect, tapered wing effect, and swept wing effect. After detailed analysis presented in the appendix, both S1223 and S1210 airfoils met the requirements. However, the airfoil S1210 was chosen due to its easier manufacturability and tooling.

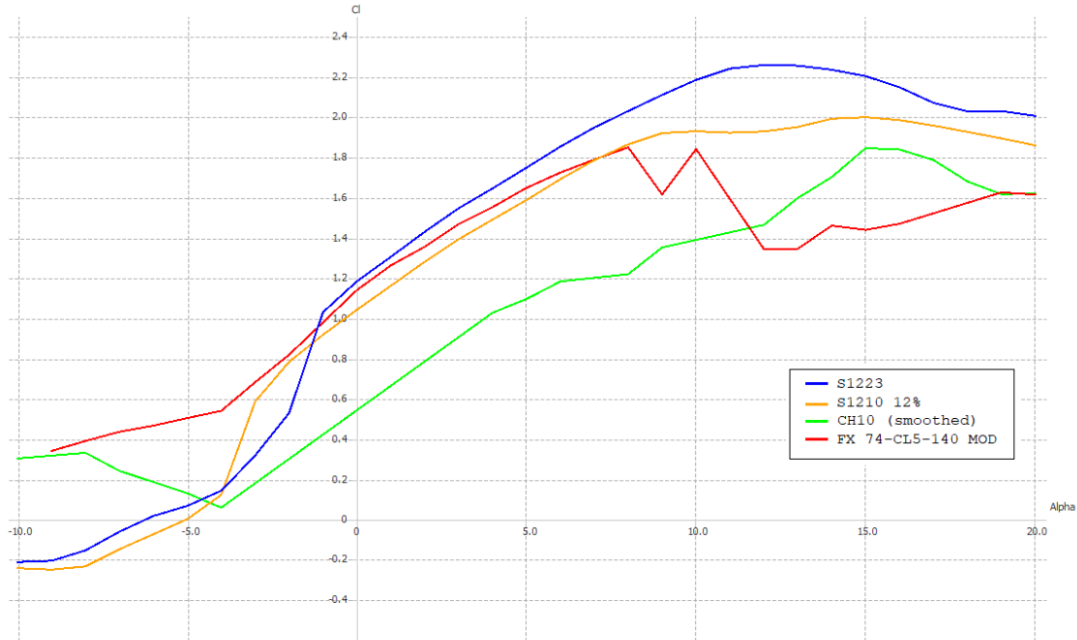


Figure 4.3 - CL in dependence of attack angle for various airfoils,  $Re = 1,4418 \cdot 10^5$

#### 4.1.2 LIFT DEVICES AND CONTROL SURFACES

To ensure enough lift during take-off and landing, flap mechanism was chosen. The complete process for lift devices sizing is done according to [1]. Lift delta calculation needed for both phases, in its pure form, is calculated as:

$$\Delta(C_{Lmax})_{TO} = 1.05 * ((C_{Lmax})_{TO} - (C_{Lmax})_{cruise}) = 0.315$$

$$\Delta(C_{Lmax})_L = 1.05 * ((C_{Lmax})_L - (C_{Lmax})_{cruise}) = 0.315$$

The aircraft has both flaps and ailerons. According to experience and recommendations, outer third of wing's trailing edge is dedicated for ailerons, whereas inner two thirds are for flaps. Both flaps and ailerons are positioned at 30 % chord from trailing edge along wingspan. The chosen flap type is *single slotted*. After imposing corrections due to tapered wing and local lift coefficient for  $\alpha=0^\circ$ , final lift delta for take-off and landing is:

$$\Delta(C_{L\alpha=0})_{TO} = 0.433$$

$$\Delta(C_{L\alpha=0})_L = 0.433$$

Now, the complete wing with flaps is analyzed in *Xflr5* for a range of flap deflections ( $\delta = 10^\circ, 0^\circ, 10^\circ, 20^\circ, 30^\circ$ ) (Figure 4.4). The results are shown in Figure 4.5. It is obvious that the analyzed wing can achieve desired lift coefficient increases for deflections  $\delta = 20^\circ$  and  $\delta = 30^\circ$ . Exact increase in lift is given below:

$$\Delta(C_{L\alpha=0})_{TO} = 0.54, \text{ for } \delta = 20^\circ$$

$$\Delta(C_{L\alpha=0})_L = 0.60, \text{ for } \delta = 30^\circ$$

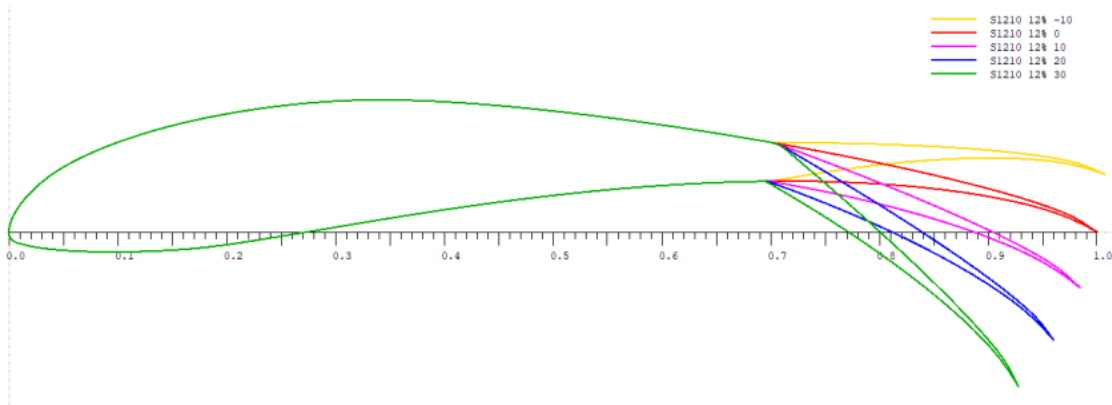


Figure 4.4 - Flap deflection positions

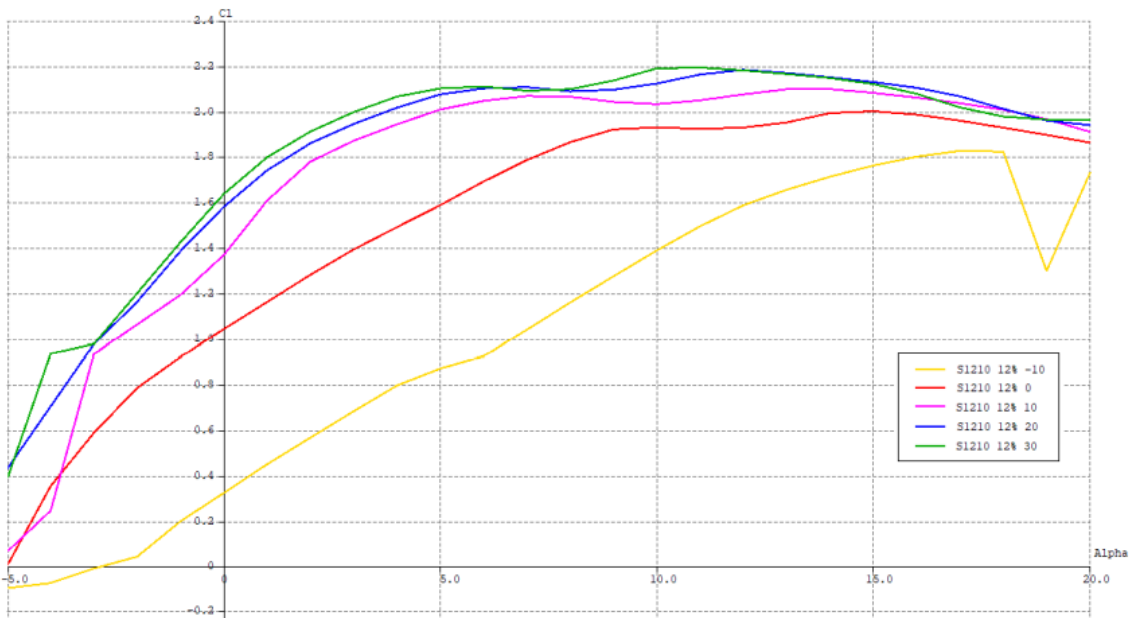


Figure 4.5 –  $C_L$  in dependency of  $\alpha$  for various flap deflections

### 4.1.3 NUMERICAL ANALYSIS

Due to the specific geometry of *blended-wing* aircraft, the fuselage is also analyzed as a part of lifting surface. Lifting surface then consists of wing and fuselage and its geometry is given in Figure 4.6. Fuselage details are given in section *Structural Design*. First, the CAD model is generated in *Solidworks* and later imported to *Xflr5* and *OpenFOAM* for analysis. The *Xflr5* analysis is based on *Lifting Line Theory (LLT)* [9] and *Panel Method* [10]. *OpenFOAM* calculation is based on *RANS equations*. The goal of both analyses is to obtain aerodynamics coefficients, and details behind them and their comparison is given in the appendix.



Figure 4.6 - Fuselage and wing geometry

Results for both *LLT* and *RANS* calculations show that lift coefficients are similar, but drag coefficients vary significantly. This is due to *RANS'* method incapability of successfully accounting viscous drag. After imposing corrections, aerodynamic coefficients for both methods ( $V=30\text{ m/s}$ ,  $\alpha=0^\circ$ ) are given in the Table 8 . Now it can be seen that both methods produce fairly similar results.

Table 8 - Aerodynamic coefficients

<b><i>Xflr5 LLT</i></b>	<b><i>OpenFOAM RANS</i></b>
$C_L = 0.717$	$C_L = 0.6772380$
$C_D = 0.0180496$	$C_D = 0.01701589$
$C_L/C_D = 39.72387199$	$C_L/C_D = 39.800332$

#### 4.1.4 BLENDED-WING OVERVIEW

The final blended-wing parameters are given in Table 9.

Table 9 - Wing parameters

<b>Wingspan <math>b</math></b>	2.4 m
<b>Projected surface (wing+fuselage)</b>	0.473 m <sup>2</sup>
<b>Projected surface (wing only)</b>	0.3932 m <sup>2</sup>
<b>Aspect ratio <math>AR</math></b>	12.166
<b>Wing taper ratio <math>\lambda</math></b>	0.6
<b>Fuselage root chord <math>c_f</math></b>	0.555 m
<b>Root chord <math>c_r</math></b>	0.2 m
<b>Wingtip chord <math>c_t</math></b>	0.12 m
<b>Leading edge sweep angle <math>\Lambda_{LE}</math></b>	10.31°
<b>Trailing edge sweep angle <math>\Lambda_{TE}</math></b>	5.68°
<b>Quarter chord line sweep angle <math>\Lambda_{c/4}</math></b>	9.36°
<b>Airfoil</b>	S1220 12%
<b>Lift device</b>	Flaps
<b>Flap position</b>	30% from trailing edge, along wingspan
<b>Aileron position</b>	30% from leading edge, along wingspan

## 4.2 TAIL DESIGN

As mentioned before, tail configuration is twin-boom, inverted V, due to improved stability and lighter construction. Based on blended-wing geometry discussed before, and center of gravity calculation given in Section 5, tail sizing is based on volumetric coefficients as shown in [1]. Figure 4.7 shows visualization of horizontal and vertical surfaces for V tail, while Figures Figure 4.8 and Figure 4.9 show final tail geometry. Table 10 - Tail parameters contains all important tail parameters.

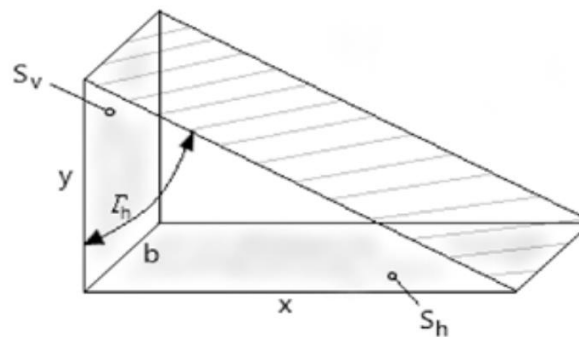


Figure 4.7 - "Butterfly angle"  $\Gamma_h$  and tail surface projections



Figure 4.8 - Tail geometry, isometric and side view

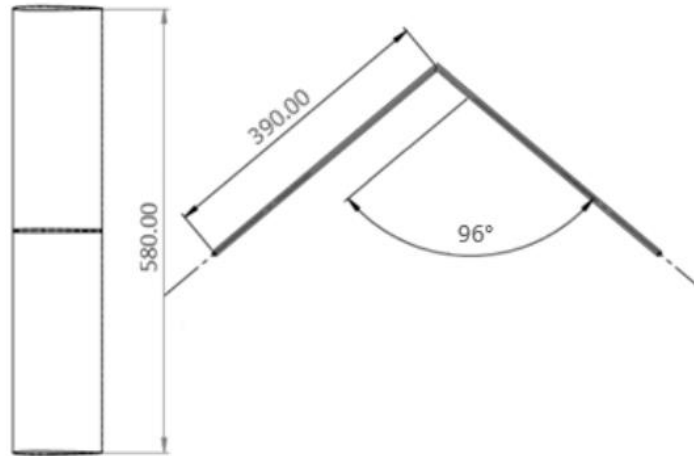


Figure 4.9 - Tail geometry, front and top view

Table 10 - Tail parameters

Horizontal tail surface area	0.05354 m <sup>2</sup>
Horizontal tail surface chord length	0.185 m
Horizontal tail surface span	0.29 m
Airfoil	NACA 0010
Vertical tail surface area	0.0950 m <sup>2</sup>
Vertical tail surface height	0.260 m <sup>2</sup>
"Butterfly angle" $\Gamma_H$	48°
Control surface position	0.0555 m
Taper ratio	1
Sweep angle	0°

## 5. CENTER OF GRAVITY

---

To determine the center of gravity, the mass of empty aircraft needs to be calculated first. The aircraft is completely made from CFRP, while laminate thickness is determined from the experience. The references are former aircraft that competed at Air Cargo Challenge competitions such as *HUSZ Tern*[11] and *HUSZ Jaeger* [12]. Mass of the main components of the aircraft are given in the table in appendix.

Center of gravity is obtained in *Solidworks* by defining the density for each component, which generated moments of inertia and total mass. With geometry manipulation of aircraft parts, the center of gravity is obtained in desired region – inside the thickest part of fuselage, where the payload will be placed. This ensures that CG will change minimally, regardless of payload mass. The CG for each component is given in the table

Table 11 - CG for each component

Component	X coordinate [m]	Y coordinate [m]	Z coordinate [m]
<i>Fuselage</i>	0	0.01356	0.27170
<i>Wing</i>	0	0.0029	0.196
<i>Tail</i>	0	0.12	-0.22
<i>Torsion box</i>	0	0.03265	0.3137
<i>Spar</i>	0	0.03275	0.22096
<i>Frames</i>	0	0.0309	0.2239
<i>Boom</i>	0	0.04	-0.05
<i>Battery</i>	0	-0.00392	0.4585
<i>Motor+propeller</i>	0	0	0.026
<i>Landing gear (mid part)</i>	0	-0.02	0.24
<i>Landing gear (front part)</i>	0	-0.1	0.47
<i>Automated measuring equipment</i>	0	0	0.435

Finally, aircraft CG position is:

$$x_{CG} = 0 \text{ m}$$

$$y_{CG} = 0.02 \text{ m}$$

$$z_{CG} = 0.23 \text{ m}$$

CG position in top, front, and side view of the aircraft are given in the appendix.

## 6. STABILITY ANALYSIS

---

### 6.1 LONGITUDINAL STABILITY

To check if the aircraft is longitudinally aerodynamically stable, according to [1] it is necessary to define the position of aerodynamic center and compare it to the center of gravity obtained in the section before. If the aircraft with the proposed tail satisfies the stability requirements, the next step is to check the static margin, which, for this aircraft, is intended to be 10 %.

The basis equation for obtaining aerodynamic center is:

$$\bar{x}_{acA} = \frac{\bar{x}_{acWf} + \frac{C_{L\alpha h}}{C_{L\alpha Wf}} \left(1 - \frac{d\varepsilon}{d\alpha}\right) \frac{S_h}{S} \bar{x}_{ach}}{1 + \frac{C_{L\alpha h}}{C_{L\alpha Wf}} \left(1 - \frac{d\varepsilon}{d\alpha}\right) \frac{S_h}{S} \bar{x}_{ach}} \quad (4)$$

where  $\bar{x}_{acWf}$  represents aerodynamic center of blended-wing,  $\bar{x}_{ach}$  represents aerodynamic center of horizontal stabilizer, and  $\frac{d\varepsilon}{d\alpha}$  is airflow binding coefficient.  $C_{L\alpha Wf}$  and  $C_{L\alpha h}$  are lift gradients for blended-wing, and horizontal stabilizer respectfully.

Aerodynamic center of horizontal stabilizer is obtained from *Xflr5* :

$$\bar{x}_{ach} = 4.7315$$

On the other hand, aerodynamic center of the blended-wing consists of wing aerodynamic center and fuselage effect on aerodynamic center:

$$\bar{x}_{acWf} = \bar{x}_{acW} + \Delta\bar{x}_{acf}$$

While wing aerodynamic center is located at  $\frac{1}{4}$  of the mean aerodynamic chord of the wing,  $\bar{c} = 0.16$ .

Fuselage effect on the aerodynamic center is calculated as:

$$\bar{x}_{acf} = \frac{\frac{dM}{d\alpha}}{qS\bar{c}C_{L\alpha W}} \quad (5)$$

Where  $\frac{dM}{d\alpha}$  is calculated as suggested in [1] , whereas lift gradient in dependance of angle of attack is calculated by equation 6:

$$C_{L\alpha} = \frac{2\pi AR}{2 + \sqrt{4 + \left(\frac{2\pi AR}{c_{l\alpha}}\right)^2 \left(1 + \frac{\tan^2 \Lambda_{c/2}}{\beta^2}\right)}} \quad (6)$$

Where  $\beta$  represents compressibility coefficient:

$$\beta = \sqrt{1 - Ma^2} \quad (7)$$

Equation 6 is used to calculate lift gradients for wing, horizontal stabilizer, and vertical stabilizer. Coefficient  $c_{l\alpha}$  is obtained from *Xflr5* for their designated airfoils.

### 6.1.1 WING LIFT GRADIENT

Input parameters for wing lift gradient equation (equation 5), without fuselage, are:

- AR=14.65
- $c_{l\alpha}=4.56 \text{ rad}^{-1}$
- $\Lambda_{c/2}=9.36^\circ$

Finally, lift coefficient gradient for wing is:

$$C_{L\alpha Wf} = 4.104 \text{ rad}^{-1}$$

### 6.1.2 HORIZONTAL AND VERTICAL STABILIZER LIFT GRADIENTS

Horizontal stabilizer lift gradient can be also obtained with equation 5. Input parameters are:

- AR=3.085
- $c_{l\alpha}=5.73 \text{ rad}^{-1}$
- $\Lambda_{c/2}=0^\circ$

Lift coefficient gradient for horizontal stabilizer is:

$$C_{L\alpha h} = 3.2688 \text{ rad}^{-1}$$

Vertical stabilizer input parameters are:

- AR=1.270
- $c_{l\alpha}=5.71 \text{ rad}^{-1}$
- $\Lambda_{c/2}=0^\circ$

Lift coefficient gradient for horizontal stabilizer is:

$$C_{L\alpha v} = 1.1239 \text{ rad}^{-1}$$

## 6.2 DIRECTIONAL STATIC STABILITY

To check the directional static stability, it is needed to determine yaw moment gradient over sideslip angle  $\beta$ . The model is based on stability analysis from [1], while basis equation is:

$$C_{n\beta} = C_{n\beta f} + C_{n\beta v} + C_{n\beta w} \quad (8)$$

- $C_{n\beta W} = 0$  – yaw moment gradient due to wing (negligible)
- $C_{n\beta v}$  - yaw moment gradient due to vertical stabilizer
- $C_{n\beta f}$  - yaw moment gradient due to fuselage

Equations used for yaw moment gradients for vertical stabilizer and fuselage are:

$$C_{n\beta v} = k_v C_{L\alpha v} \left(1 + \frac{d\sigma}{d\beta}\right) \eta_v \frac{S_v l_v}{S b} \quad (9)$$

$$C_{n\beta f} = -57.3 K_N K_{Re} \frac{S_{fs} l_f}{S b} \quad (10)$$

where parameters are defined as:

- $k_v = 1$  – empirical factor for assuming yaw moment
- $\left(1 + \frac{d\sigma}{d\beta}\right) \eta_v$  – model that defines airflow binding
- $l_v$  – distance from aerodynamic center to CG
- $K_N = 0$  – empirical factor
- $K_{Re}$  – Reynolds number effect on directional static stability
- $S_{fs}$  – side projection area of fuselage
- $l_f$  – fuselage length

### 6.3 RESULTS

Obtained aerodynamic center of the aircraft is:

$$\bar{x}_{ac} = 0.458 \text{ m}$$

As the aircraft is designed to have a constant CG, because payload is always placed along the same CG line inside the payload area, it is unaffected by various payload weights. Thus, only one analysis for static margin is needed. Figure 6.1 shows different aerodynamic center positions, for 10% static margin and obtained horizontal stabilizer from the report. It shows that the tail satisfies longitudinal stability requirements. Moreover, the horizontal stabilizer area can even be reduced further.

On the other hand, total yaw moment gradient needed is:

$$C_{n\beta} = 0.001 \text{ 1/}^\circ$$

Figure 6.2 shows that designed vertical stabilizer produces  $C_{n\beta} = 0.00108 \text{ 1/}^\circ$  which also meets the stability requirements.

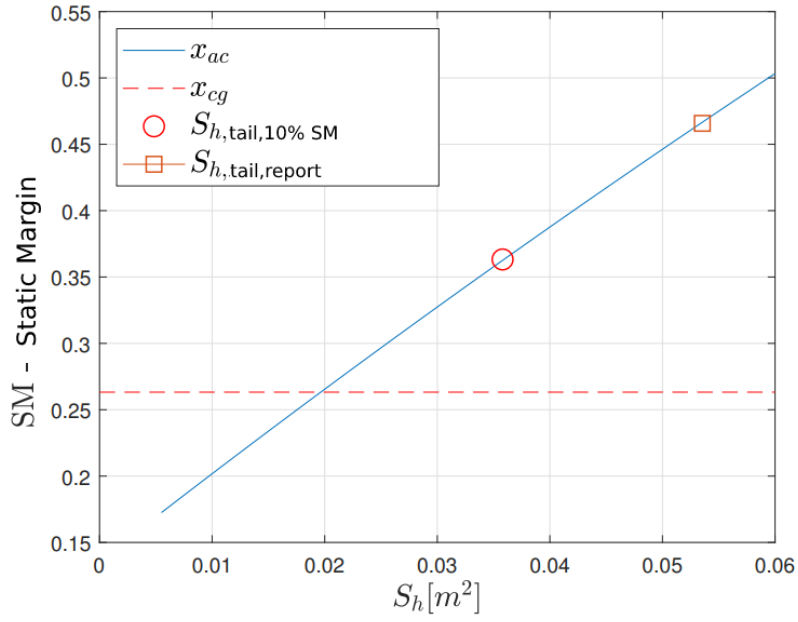


Figure 6.1 - Static margin

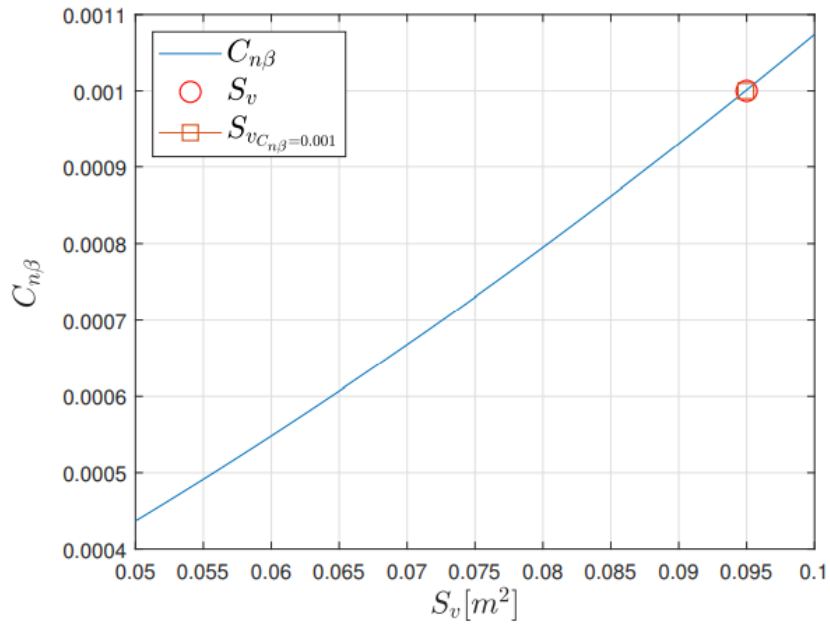


Figure 6.2 - Directional static stability analysis

## 7. STRUCTURAL DESIGN

---

This section deals with structural analysis and mass estimation of various components of the aircraft. The construction design is based on manufacturing experience, and analytical and numerical (*Abaqus FEA*) methods.

The fuselage is made of one lamina of 20 g/m<sup>2</sup> bi-directional carbon fabric, one lamina of *AIREX* 1.2 mm foam, and one lamina of 68 g/m<sup>2</sup> *TeXtreme* carbon fabric.

Wings and tail are made of one lamina of 40 g/m<sup>2</sup> bi-directional carbon fabric, one lamina of *AIREX* 1.2 mm foam, and one lamina of 20 g/m<sup>2</sup> bi-directional carbon fabric. Ailerons and flaps are made similarly, but without the 20 g/m<sup>2</sup> lamina.

The main bending load elements are spars, which are positioned along the wingspan, made of *CFRP* telescopic tubes. Numerical calculations have shown that main spar dimensions of 18/16 mm, in combination with 16/14 mm and 14/10 mm will suffice. Wings also have secondary spars at the transition to flaps/ailerons, also made from *CFRP*. The spars connect at the fuselage and are reinforced with uni-directional carbon fiber, as the loads have the highest values there.

For fuselage torsion, frames made from bought *CFRP* panels are used, as well for wing root parts and tail. However, for thinner wing areas, and for flaps and ailerons, homemade *GFRP* frames are used.

Two booms that connect tail and wings are made of *CFRP* tubes.

The aircraft is divided into sections, to fit inside a transportation box. Those sections are:

- Fuselage
- Two wings with flaps and ailerons
- Two booms
- Tail

All parts are designed to connect via bought *CFRP* tubes that fit inside spars, for connecting fuselage and wings, or booms, for connecting tail, booms, and wings.

### 7.1 FUSELAGE

The inner area of the fuselage is dedicated for payload placement, directly under the wings, whereas frontal area is reserved for battery and automated measuring equipment. The payload and components are placed inside the fuselage through the opening at the upper surface of the fuselage. Cargo area details are given in the appendix B. During the flight, the opening is covered by *CFRP* lid, and the payload is secured with harnesses. Payload area is enclosed by *CFRP* and *GFRP* frames, while the frontal frame has enough space to fit in a main battery, additional battery, and automated measuring equipment. Also, between frontal and inner area, is a place for connecting both wing spars. At the back of the fuselage is motor placement (pusher

configuration). The fuselage structure is shown in Figure 7.1. and Figure 7.2, and wing structures are shown in Figure 7.3.

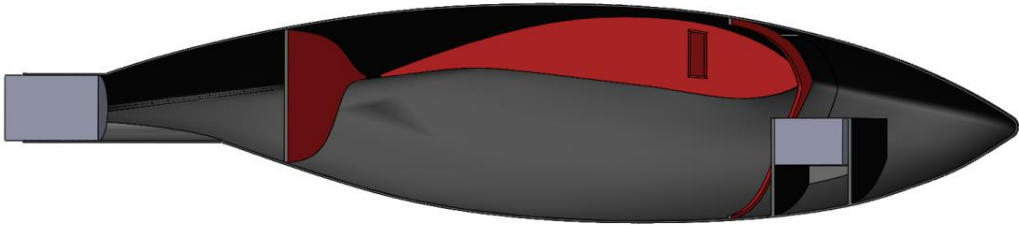


Figure 7.1 - Fuselage structure

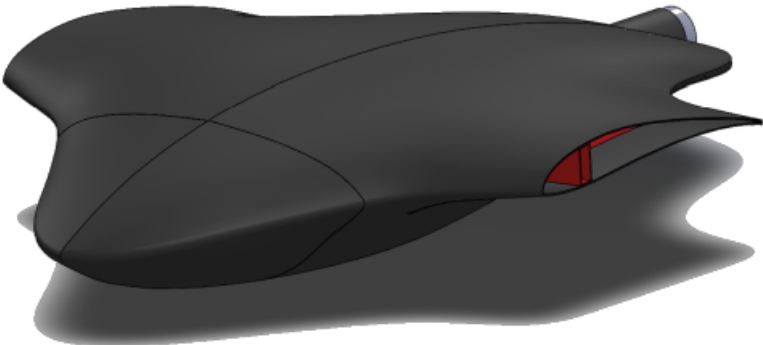


Figure 7.2 - Fuselage

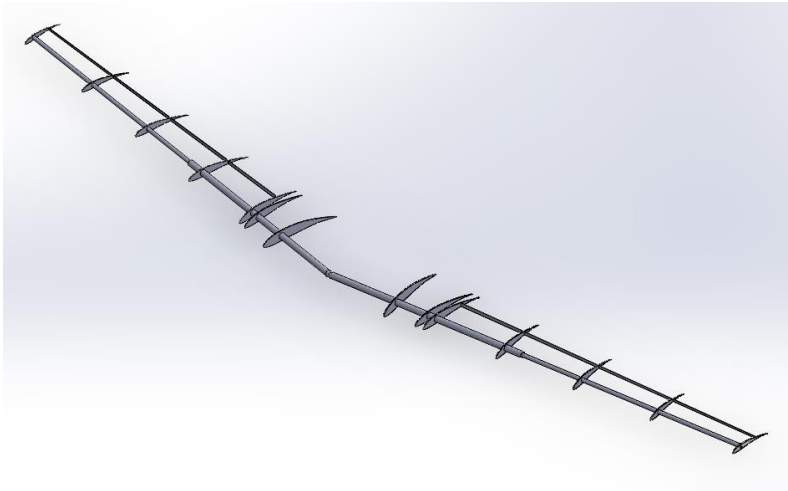


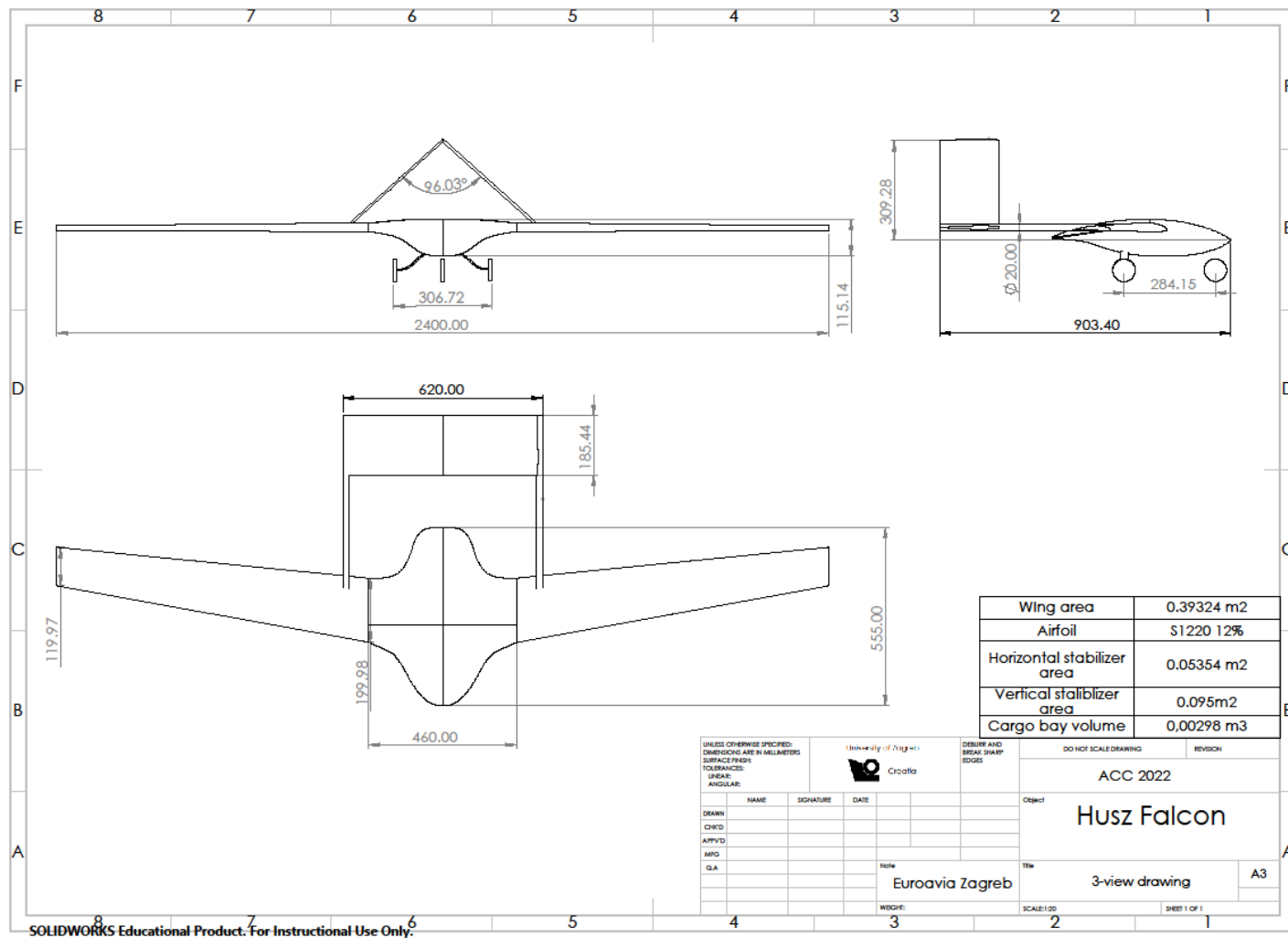
Figure 7.3 - Wing structure

## 8. OUTLOOK

---

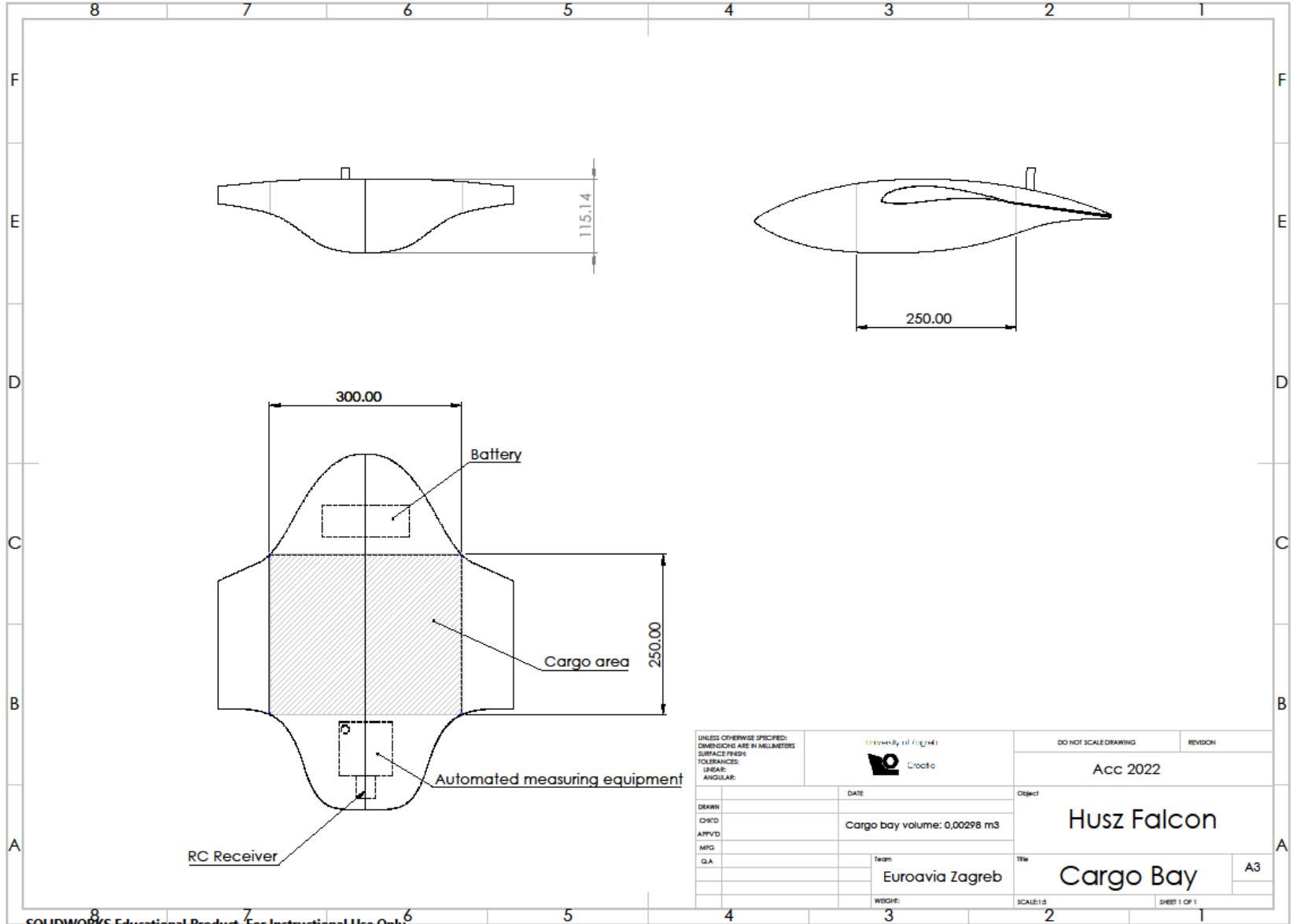
New regulations resulted in taking new approach to the aircraft design as presented in this report. The team decided to settle on blended-wing configuration, with swept wings, which the team from Zagreb is not experienced with. Nevertheless, the complete design phase was consistent with goals presented at the beginning of the report and has been supported by numerical simulations. The team had some problems during the preliminary design, as the blended-wing configurations are not common, and methods for their sizing are still not standardized. The biggest issue the team is probably going to have is during the manufacturing process due to uncommon geometries. Also, swept wings are sensitive to CG position, which additionally increases requirements for precise production.

# APPENDIX A – DRAWINGS



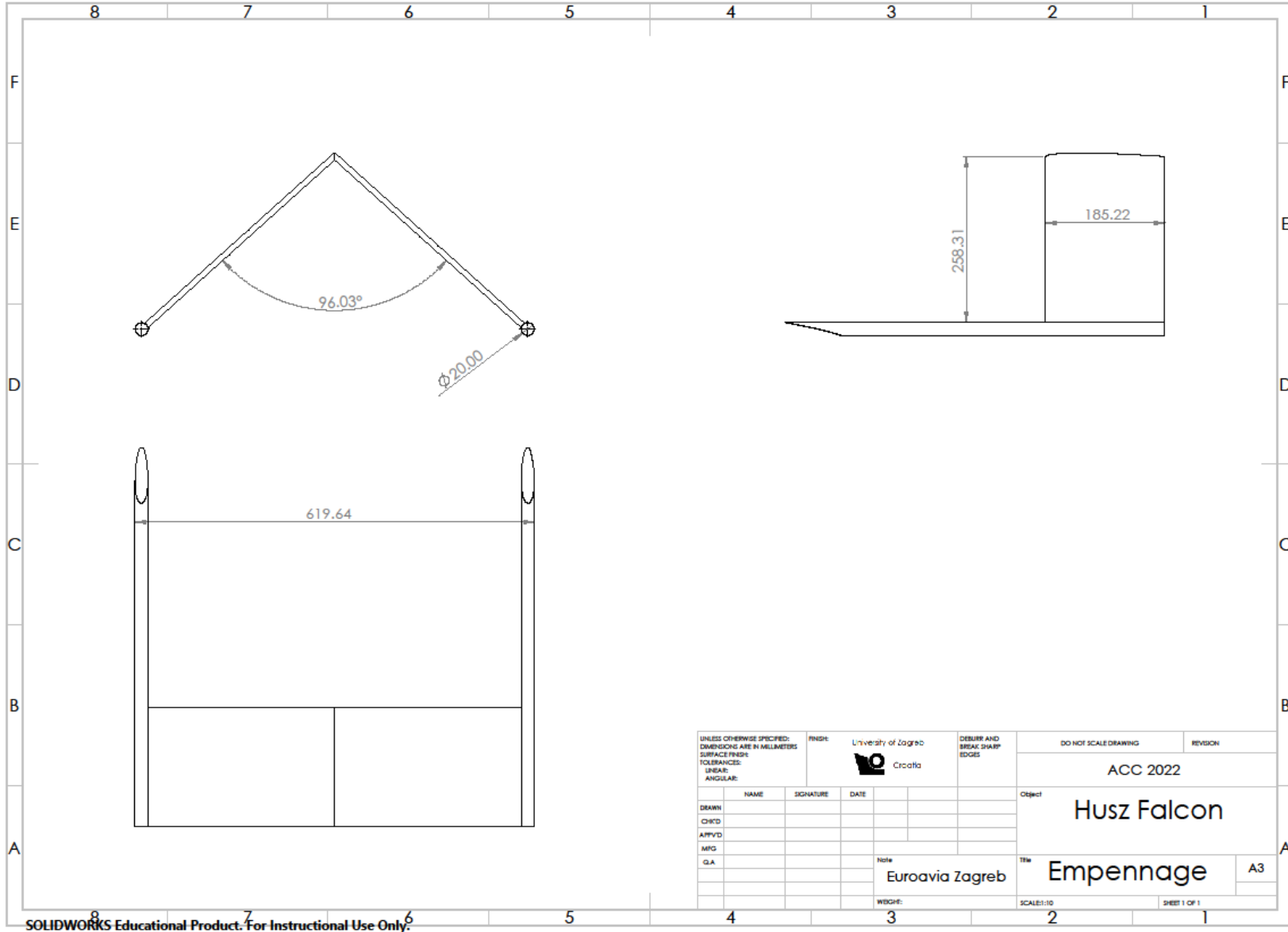
SOLIDWORKS Educational Product. For Instructional Use Only.





UNLESS OTHERWISE SPECIFIED: DIMENSIONS ARE IN MILLIMETERS SURFACE FINISH: TOLERANCES: LINEAR: ANGULAR:		University of Zagreb Croatica		DO NOT SCALE DRAWING		REVISION	
		DATE		Acc 2022			
DRAWN		Cargo bay volume: 0,00298 m3		Object			
CHK'D				Husz Falcon			
APP'VD				Title			
MFG		Team		Cargo Bay			
QA		Euroavia Zagreb		A3			
		WEIGHT:		SCALE:1:5		SHEET 1 OF 1	

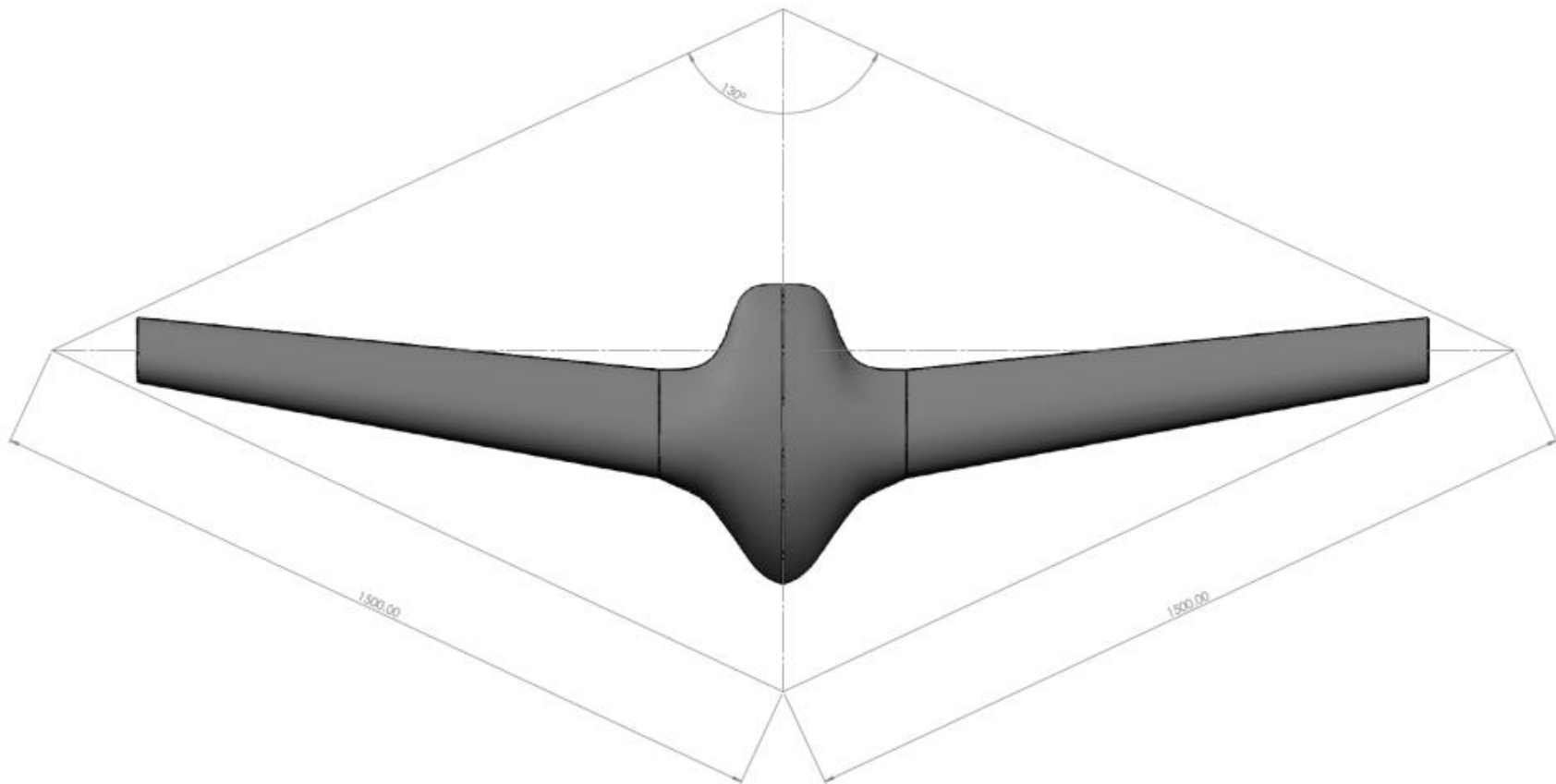
SOLIDWORKS Educational Product. For Instructional Use Only.



SOLIDWORKS Educational Product. For Instructional Use Only.

## APPENDIX B – BOUNDING BOX

---



## APPENDIX C – ADDITIONAL WEIGHT DATA

Table 12 - Mass of main components

<b>Component</b>	<b>Mass [kg]</b>
<i>Fuselage</i>	<i>0.502</i>
<i>Wing</i>	<i>0.343</i>
<i>Tail</i>	<i>0.08</i>
<i>Torsion box</i>	<i>0.215</i>
<i>Spar</i>	<i>0.175</i>
<i>Frames</i>	<i>0.022</i>
<i>Boom</i>	<i>0.4</i>
<i>Battery</i>	<i>0.493</i>
<i>Motor+propeller</i>	<i>0.197</i>
<i>Landing gear</i>	<i>0.22</i>
<i>Servo motors</i>	<i>0.036</i>
<i>Automated measuring equipment</i>	<i>0.15</i>
<i>Other (electronics, nuts, wiring, etc.)</i>	<i>0.212</i>

Table 13 - Similar aircraft mass weight data

<b>Aircraft</b>	<b><math>W_E</math> [kg]</b>	<b><math>W_{TO}</math> [kg]</b>
MyFlyDream MFD	4	5.5
Believer	3.8	5.5
LAGARI 2018	3.5	9.4
Swallow Electric UAV	3.3	9
Bumble Bee	1.6	3.6
DBF 2006	2.5	6.9

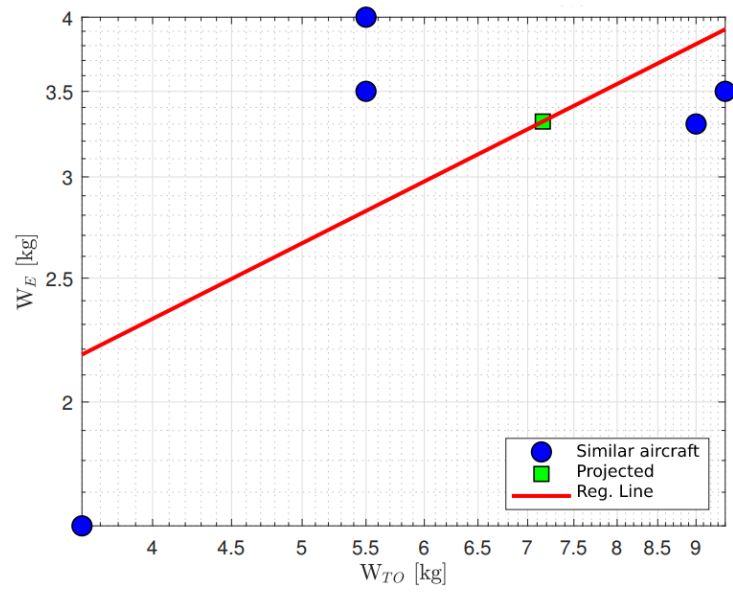


Figure 0.1 - Projected empty weight

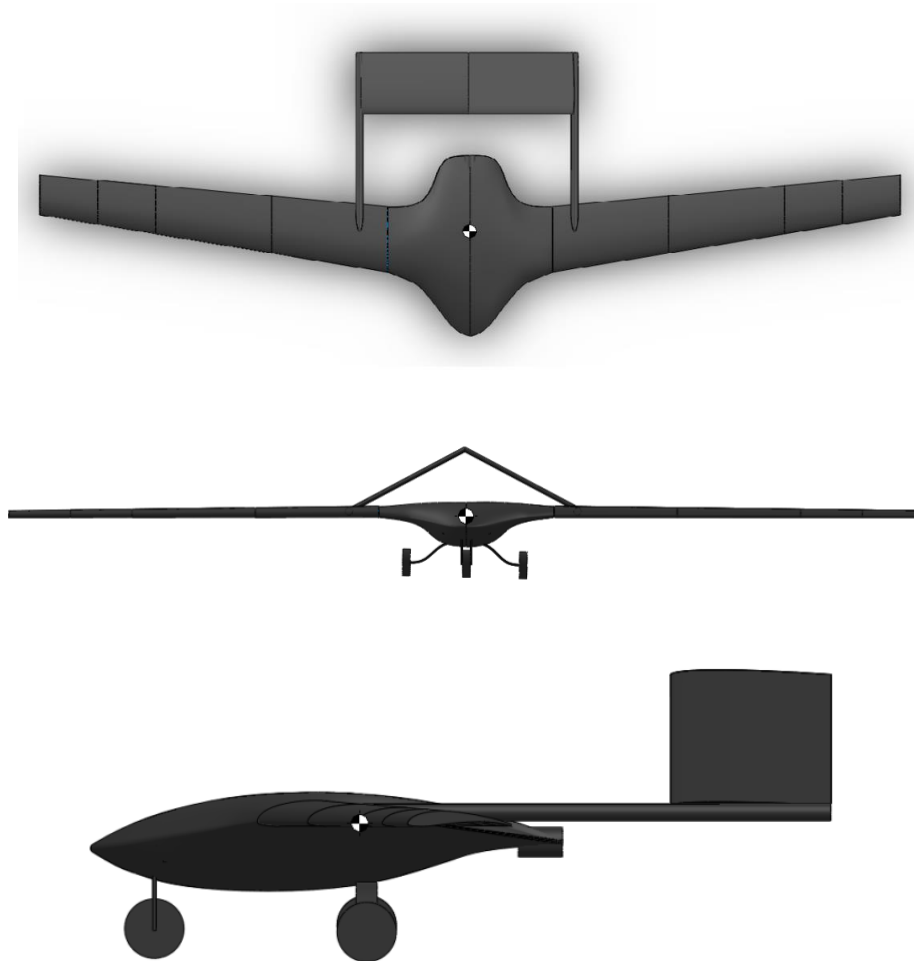


Figure 0.2 - CG position in top, front, and right vie

# APPENDIX D – NUMERICAL RESULTS

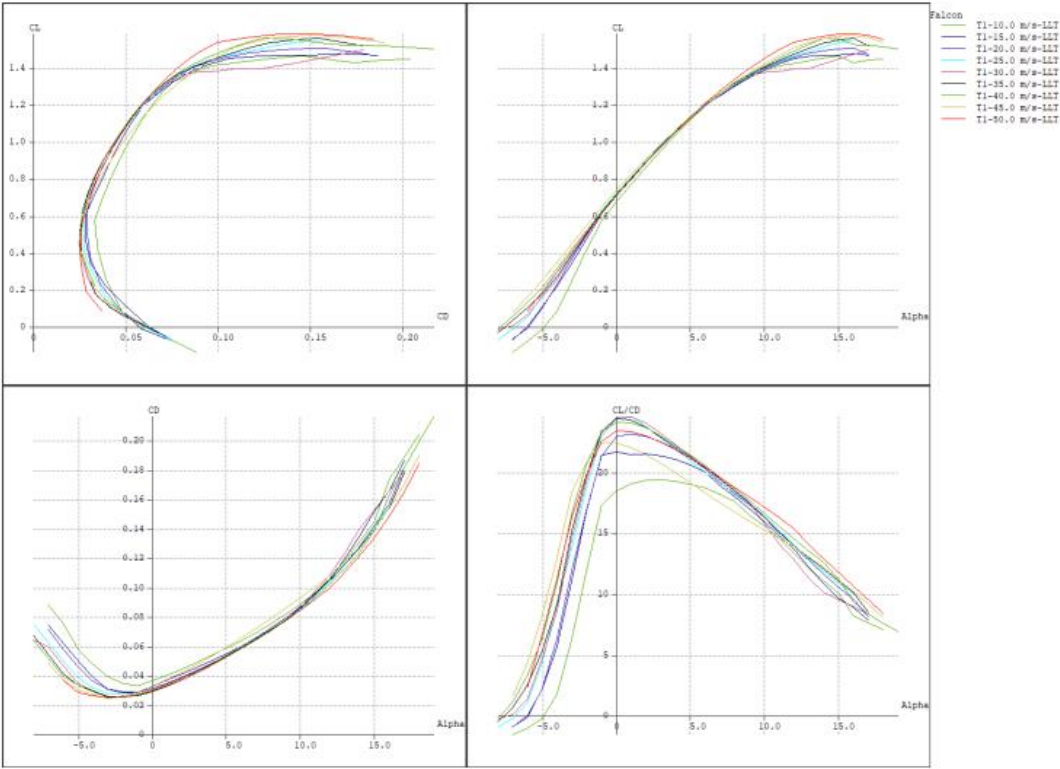


Figure 2 - LLT method result

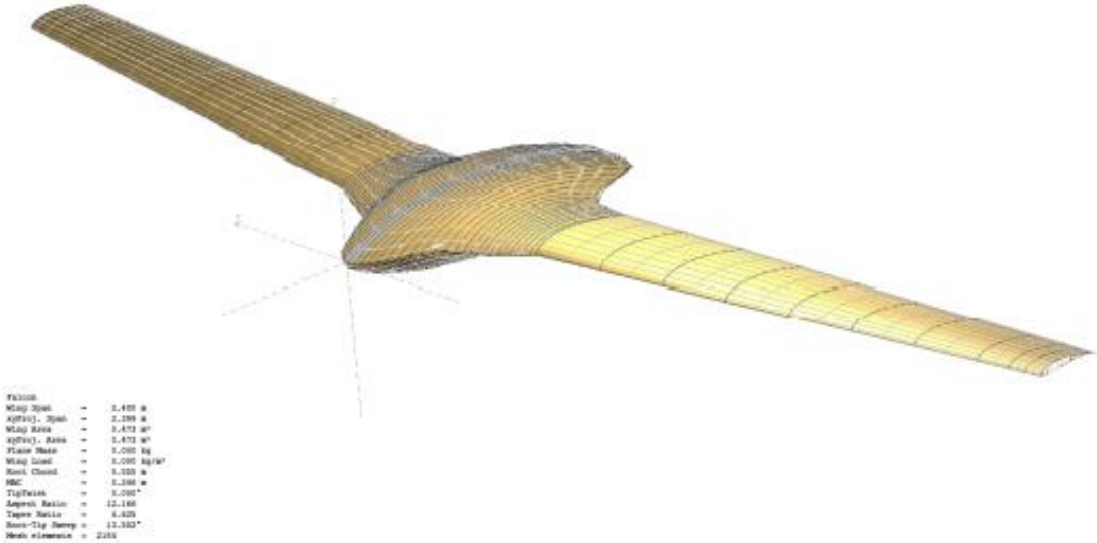


Figure 3 - Xflr5 geometry



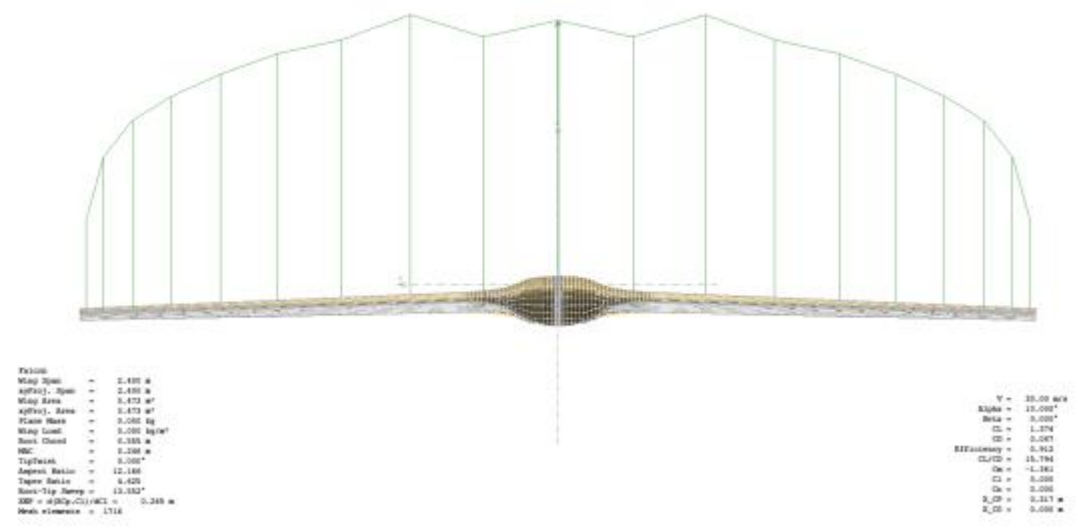
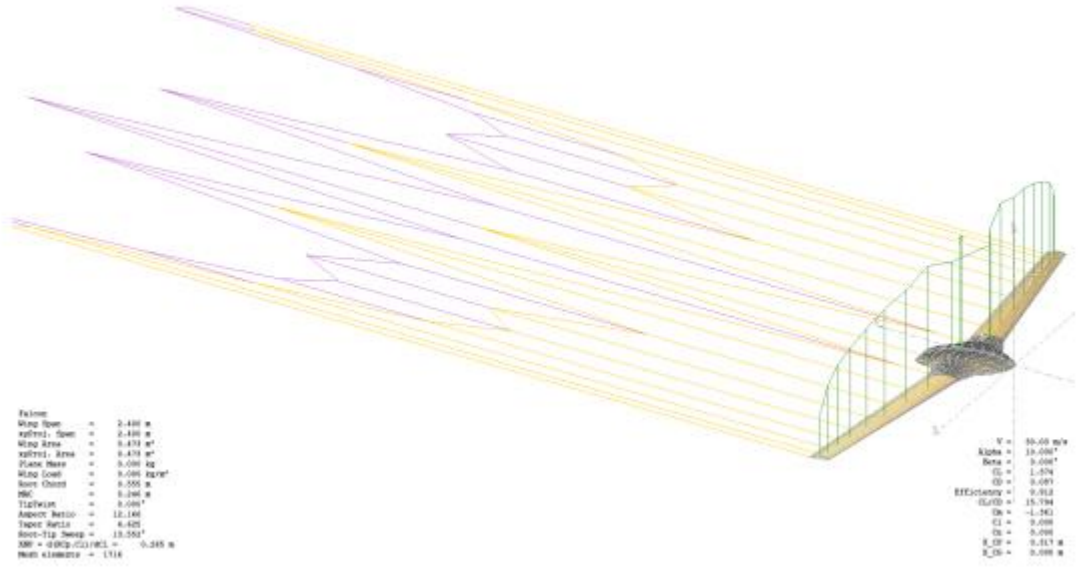


Figure 5 - LLT, 30 m/s,  $\alpha=10^\circ$

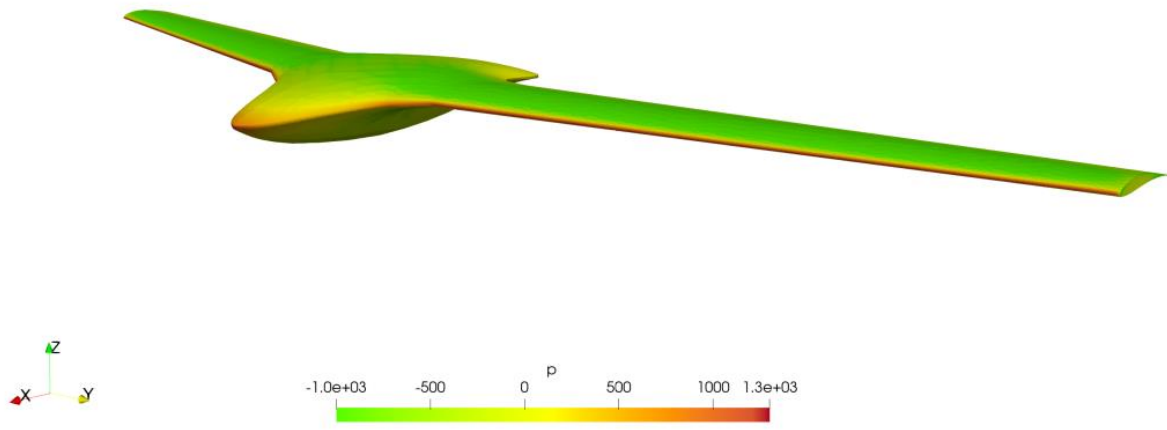


Figure 6 - CFD, pressure field on aircraft surface

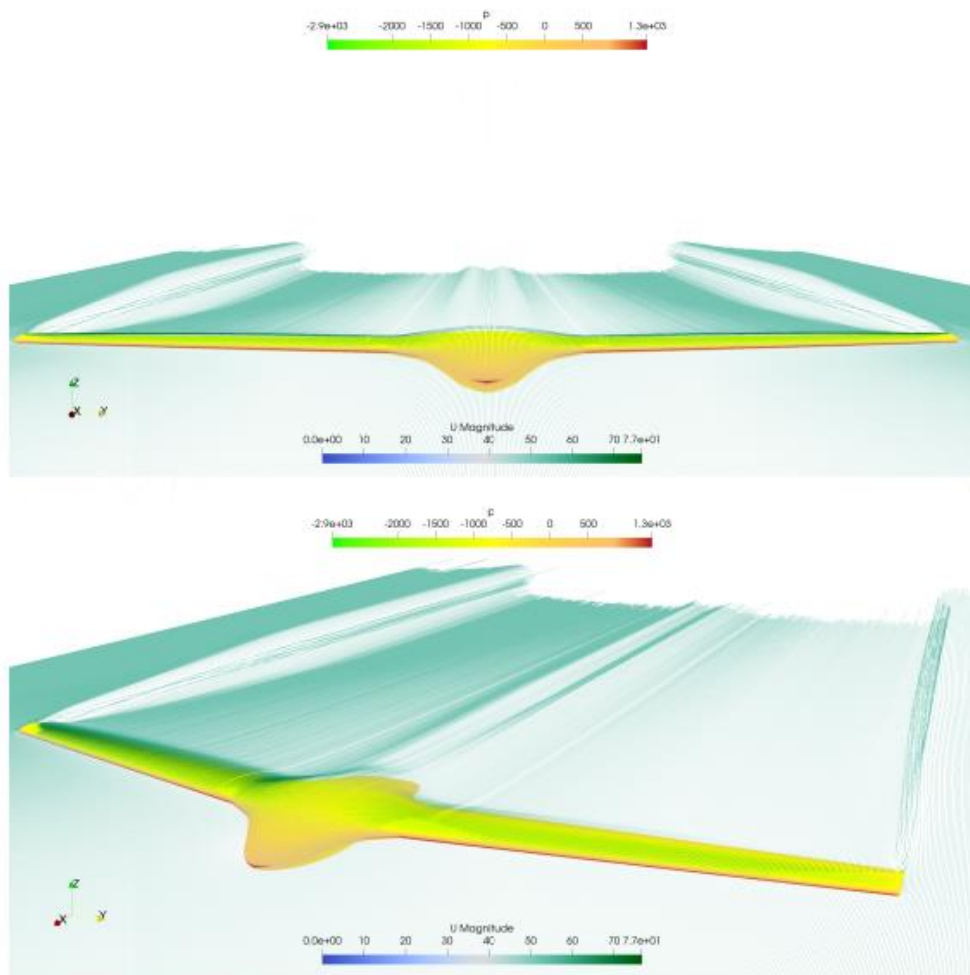


Figure 7 - CFD, velocity field



## BIBLIOGRAPHY

---

- [1] Roskam J., Airplane Design: Part I: Preliminary sizing of airplanes
- [2] Golden, Bruce L., Edward A. Wasil, and Patrick T. Harker. "The analytic hierarchy process." Applications and Studies, Berlin, Heidelberg 2 (1989).
- [3] Modelmotors, AXI 2826/10 GOLD LINE V2, accessed 29.04.2022.  
<https://www.modelmotors.cz/product/detail/394/>
- [4] Zeee, Zeee Lipo Battery 11.1V 8000mAh 100C 3S, accessed 29.04.2022.  
<https://zeeebattery.com/products/zeee-lipo-battery-111v-8000mah-100c-3s-lipo-battery-with-deans-plug-for-rc-car-truck-rc-truggy-fpv-airplane-boat-buggy-254>
- [5] Roskam, Jan. "Preliminary calculation of aerodynamic, thrust and power characteristics." Airplane design 21 (1987): 213-354.
- [6] Sleeman, William C. Aerodynamic Characteristics of a Wing with Quarter-chord Line Swept Back 35°, Aspect Ratio 6, Taper Ratio 0.6, and NACA 65A006 Airfoil Section: Transonic-bump Method. National Advisory Committee for Aeronautics, 1949.
- [7] Bramantya, Muhammad Agung, and Ega Nanda Arda Janitra. "Effect taper ratio on V-tail configuration of unmanned aerial vehicle." AIP Conference Proceedings. Vol. 2403. No. 1. AIP Publishing LLC, 2021.
- [8] Drela, Mark. "XFOIL: An analysis and design system for low Reynolds number airfoils." Low Reynolds number aerodynamics. Springer, Berlin, Heidelberg, 1989. 1-12.
- [9] Phillips, Warren F., and D. O. Snyder. "Modern adaptation of Prandtl's classic lifting-line theory." Journal of Aircraft 37.4 (2000): 662-670.
- [10] Maskew, Brian. "Prediction of subsonic aerodynamic characteristics: a case for low-order panel methods." *Journal of Aircraft* 19.2 (1982): 157-163.
- [11] Pađen, Ivan. Analiza čvrstoće kompozitne ramenjače aviona za natjecanje Air Cargo Challenge. Diss. University of Zagreb. Faculty of Mechanical Engineering and Naval Architecture, 2016.
- [12] Barać, Ceilinger, Grlj, Krišto, Lončarević, Tukarić, Uroda, Zubak, Final Report from Aircraft Design I and II – Huzs Jaeger, Faculty of Mechanical Engineering and Naval Architecture, University of Zagreb, 2019.